Low driving voltage and efficient orange-red phosphorescent organic light-emitting devices based on a benzotriazole iridium complex

Zhen-Yuan Xia [a], Xiao Xiao [a], Jian-Hua Su [a,*], Chi-Sheng Chang [b], Chin H. Chen [b], Dan-Lin Li [a], He Tian [a,*]

[a] Key Laboratory for Advanced Materials and Institute of Fine Chemicals, East China University of Science & Technology, Shanghai 200237, China
[b] Display Institute, Microelectronics and Information Systems Research Center, National Chiao Tung University, Hsinchu 300, Taiwan, ROC

ARTICLE INFO

ABSTRACT

Efficient orange-red phosphorescent organic light-emitting devices (PHOLED) with various doping concentrations of benzotriazole–iridium complex [(TBT)$_2$Ir(acac)] (bis[4-(2H-benzotriazol-2-yl)-N,N-diphenyl-aniline-N^1,C^3] iridium acetylacetonate) in 4,4'-N,N'-di(carbazolyl) biphenyl (CBP) host were fabricated. The sterically hindered iridium ligands alleviate self-quenching of the phosphorescence at high doping levels. Under the optimal doping concentration of 20 wt.%, the maximum external quantum efficiency (EQE), luminance and power yield reach 9.06%, 15.81 cd/A and 13.8 lm/W, respectively. Increasing the doping concentration from 5% to 30 wt.% significantly decreases the driving voltage. The driving voltage of 30% (TBT)$_2$Ir(acac) doped device is only 3.16 V at 1 mA/cm^2 with power yield of 13.32 lm/W.

© 2009 Elsevier B.V. All rights reserved.

1. Introduction

Organic light-emitting diodes (OLEDs) have attracted much attention in recent years owing to their potential as low-cost and large-area full color displays and solid-state lightings [1]. In particular, electro-phosphorescent OLEDs (or PHOLED) have outstanding performance because they take advantage of both singlet ($\leq$25%) and triplet excitons ($\leq$75%), achieving excellent external quantum efficiency and power efficiency [2,3]. Among many organometallic complexes composed of platinum (II) [4,5], osmium (II) [6], ruthenium (II) [7], iridium (III) [8–11], the iridium ones with ligands of cyclometalated phenylpyridine and their analogues exhibit relatively short triplet excited-state lifetimes, high emission quantum yields and tunable emission wavelengths [12–14]. But color tunable iridium complexes based on ligands other than phenylpyridine derivatives have been rarely reported [15a].

In previous reports, we have designed and synthesized a series of novel iridium (III) complexes with benzotriazole derivatives ligand. It was found that color tunable properties could be realized for these phosphorescent materials [15b]. However, these complexes have not been fully investigated [16] although they have some unique advantages: first, ligand derivatization can be easily achieved by cyclization of corresponding benzohydrazide with different functional aryl groups [15], thus allowing tailor-made

physical and chemical properties such as emission color, carrier-transporting and thermal stability of the complex. Second, our preliminary MO calculations suggest that the LUMO energy levels of these ligands are largely contributed by benzotriazole and the extended π-conjugation, which results in a red-shift emission. This feature may benefit to design promising orange or red phosphorescent emitters.

In this report, we adopted bis[4-(2H-benzotriazol-2-yl)-N,N-diphenylaniline-N^1,C^3] iridium acetylacetonate [Ir(TBT)$_2$(acac)], a heteroleptic orange-red emitting iridium (III) complex in phosphorescent OLED. The complex possesses good morphological and thermal stability, strong orange-red phosphorescence and matched energy levels with commonly used host CBP in PHOLED. The electroluminescence devices were fabricated by doping Ir(TBT)$_2$(acac) into the CBP host with various concentrations as the emitting layer. The optimized 20 wt.% dopant device achieves maximum luminance yield and external quantum efficiencies (EQEs) of 15.81 cd/A and 9.06% at 3.59 V, respectively. Also the driving voltage decreases as the doping level increases without significantly hampering the device performance. The driving voltage at 30 wt.% dopant level is 3.16 V at a current density of 1 mA/cm^2 and only 4.85 V at a current density of 40 mA/cm^2, which is significantly lower than most of the reported orange or red phosphor with CBP host [17–19].

2. Experimental

The chemical structures of key materials and the device configuration of monochromatic PHOLED are shown in Fig. 1. The synthesis

---

* Corresponding authors. Fax: +86 21 64252288.
E-mail addresses: bbsjh@ecust.edu.cn (J.-H. Su), tianhe@ecust.edu.cn (H. Tian).
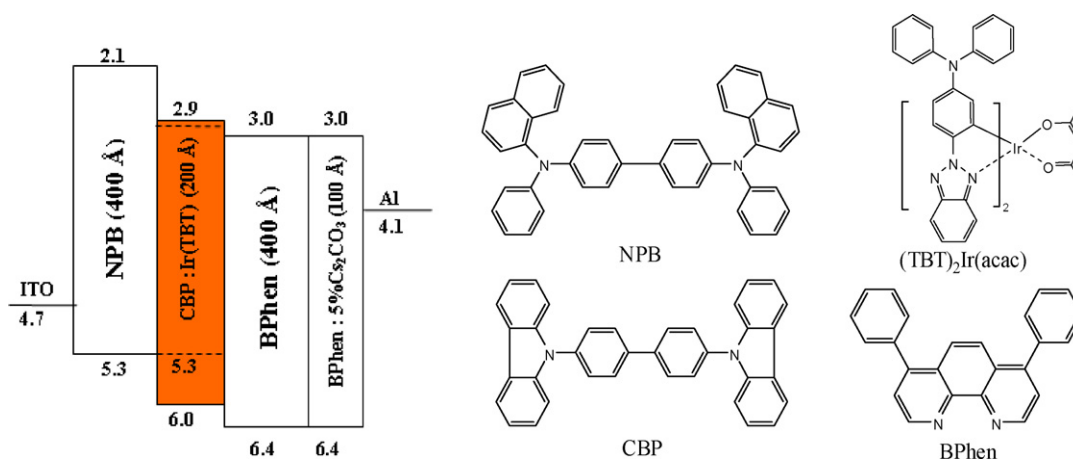
Fig. 1. Schematic energy level diagram of the orange-red PHOLED and molecular structures of relevant compounds in these devices. Numbers indicate the respective HOMO/LUMO energies of all organic materials relative to vacuum.

and characterization of Ir(TBT)$_2$(acac) have been published elsewhere [15a]. Other materials were obtained commercially and used without further purification.

Prior to the deposition of organic materials, indium-tin-oxide (ITO)/glass was cleaned with a routine cleaning procedure and pretreated with oxygen plasma. Devices were fabricated under about 10^{-6} Torr base vacuum in a thin-film evaporation coater following a published protocol [20]. The current–voltage–luminance characteristics were measured with a diode array rapid scan system using a Photo Research PR650 spectrophotometer and a computer-controlled, programmable, direct-current (DC) source.

3. Results and discussion

3.1. Photophysical and electrochemical characterization

Fig. 2 shows the photoluminescence (PL) and electroluminescence (EL) of Ir(TBT)$_2$(acac). The PL spectrum shows a peak at 598 nm and the EL spectrum at 588 nm corresponding to an orange-red emission (CIE$_{x,y}$ (0.58, 0.41)). The full width at half maximum (FWHM) is about 100 nm. The 10 nm bathochromic shift going from the EL to solution PL may be caused by the slight stabilization of the excited state by THF which is a moderately polar solvent (dielectric constant ε_0: 7.52 at 22 °C) [21].

Previous electrochemical data reveals that the highest occupied molecular orbital (HOMO) and lowest unoccupied molecular orbital (LUMO) of Ir(TBT)$_2$(acac) were -5.32 eV and -2.89 eV, respectively [15b]. The electron-withdrawing benzotriazole group lowers LUMO by increasing the parent ligand's electron affinity, while the electron-donating triphenylamine group lowers the oxidation potential and then elevates the HOMO.

3.2. Characterization of orange-red PHOLED

According to our previous report, Ir(TBT)$_2$(acac) is an amorphous and morphologically stable solid with a high glass transition temperature (T_g) of 133 °C [15b]. In order to optimize the PHOLED performance, devices with different dopant concentration were fabricated as the following structure: ITO/CF$_x$/NPB (400 Å)/CBP:x wt.% Ir(TBT)$_2$(acac) (200 Å)/Bphen (400 Å)/Bphen:Cs$_2$CO$_3$ (100 Å)/Al (1400 Å) (Fig. 1) (ITO = indium tin oxide, NPB = 4,4-bis [N-(1-naphthyl)-N-phenylamino]biphenyl, CBP = 4,4′-N,N′-di(carbazolyl) biphenyl, Bphen = 4,7-diphenyl-1,10-phenanthroline). The detailed molecular structure and device architecture have been shown in Fig. 1. The CF$_x$ acts as the hole injection layer. The NPB is the hole transport layer, CBP:x wt.% Ir(TBT)$_2$(acac) is the orange-red emissive layer (x = 5, 10, 20, 30). BPhen is the electron transportation and hole-blocking
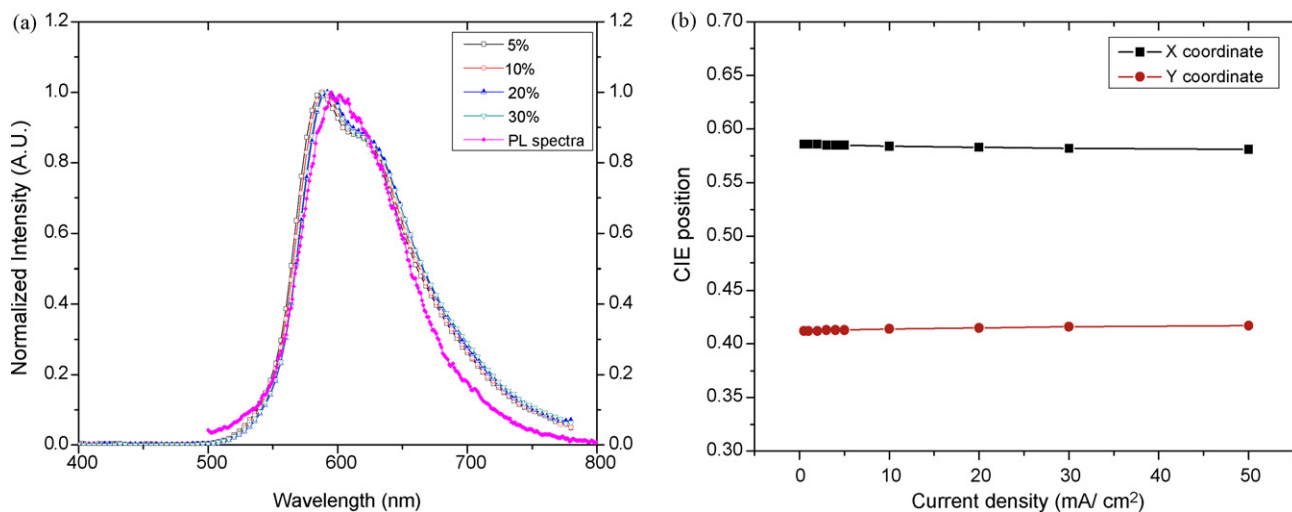
Fig. 2. (a) PL spectra of dopant Ir(TBT)$_2$(acac) in THF (10^{-5} M) at 293 K and EL spectra of the orange-red devices with various doping concentrations of Ir(TBT)$_2$(acac). (b) CIE coordinate values of 20 wt.% Ir(TBT)$_2$(acac) dopant PHOLED under different current density.

Table 1
Performance parameters of Ir(TBT)$_2$(acac)-doped orange-red PHOLED at the current density of 2 mA/cm^2.

| Con. (wt.%)	Voltage (V)	Yield (cd/A)	Efficiency (lm/W)	EQE (%)	CIE
5%	5.45	10.1	5.8	5.4	(0.57, 0.42)
10%	4.90	13.1	8.4	7.2	(0.58, 0.42)
20%	3.99	14.6	11.5	8.3	(0.59, 0.41)
30%	3.30	12.9	12.2	7.4	(0.59, 0.41)

layer. BPhen:Cs$_2$CO$_3$ is the *n*-doping layer. Finally the Al is the cathode.

As shown in Fig. 1 the schematic energy level diagram [22], the LUMO level of Ir(TBT)$_2$(acac) (LUMO: −2.89 eV) matches well with that of the host CBP (LUMO: −2.90 eV), so the energy barrier for electron injection is very small. The high bandgap CBP host guarantees no back energy transfer from dopant to host will occur. The LUMO energy gap (E_g) between the NPB/CBP interface (0.8 eV) and HOMO gap in the CBP/BPhen interface of (0.4 eV) are large enough to confine the recombination zone of electrons and holes in the emitter zone.

The luminance efficiency and EQE of Ir(TBT)$_2$(acac)-doped orange-red PHOLED at the current density of 2 mA/cm^2 are shown in Table 1. Maximum luminance yield (15.81 cd/A) and external quantum efficiency (EQE) (9.06%) are achieved under 20 wt.% doping concentration in CBP at current density of 0.5 mA/cm^2 (Fig. 3c and d). The EL spectrum exhibits a peak wavelength at 588 nm with a bright orange-red emission (CIE (0.58, 0.41)) (Fig. 4). Its CIE values remain almost constant with variation of the current density from 0.5 mA/cm^2 to 50 mA/cm^2 (Fig. 2b). The EL peak does not change

over the range of doping concentrations as well (Table 1). There is no residual emission from the host or adjacent layers under examined doping concentrations, indicating extremely efficient energy transfer to dopant (Fig. 2a). However, like most phosphorescent devices, efficiency decreases as current density increases, which has been attributed to a combination of triplet–triplet (T–T) annihilation [23] and field-induced excitons dissociation effects [24].

It is interesting that the drive voltage dramatically decreases with increasing doping concentration (Fig. 3a). It drops from 5.45 V to 3.30 V at 2 mA/cm^2 when the concentration rises from 5% to 30 wt.% without significant loss of efficiency and luminance. The driving voltage of 30 wt.% dopant device is 3.16 V at the current density of 1 mA/cm^2 and only 4.85 V at 40 mA/cm^2. Because of the lower driving voltage, The power efficiency of 30 wt.% dopant device is higher than that of 20 wt.% dopant device from 1 mA/cm^2 to 20 mA/cm^2 (Fig. 3d). Presumably this is attributed to the well-matched HOMO energy levels of Ir(TBT)$_2$(acac) (HOMO: −5.32 eV) and hole-transporting layer NPB (HOMO: −5.3 eV) (Fig. 1), thus modifying the hole inject ability of CBP host (HOMO: −6.0 eV) from the adjacent NPB layer. The high-lying HOMO energy level
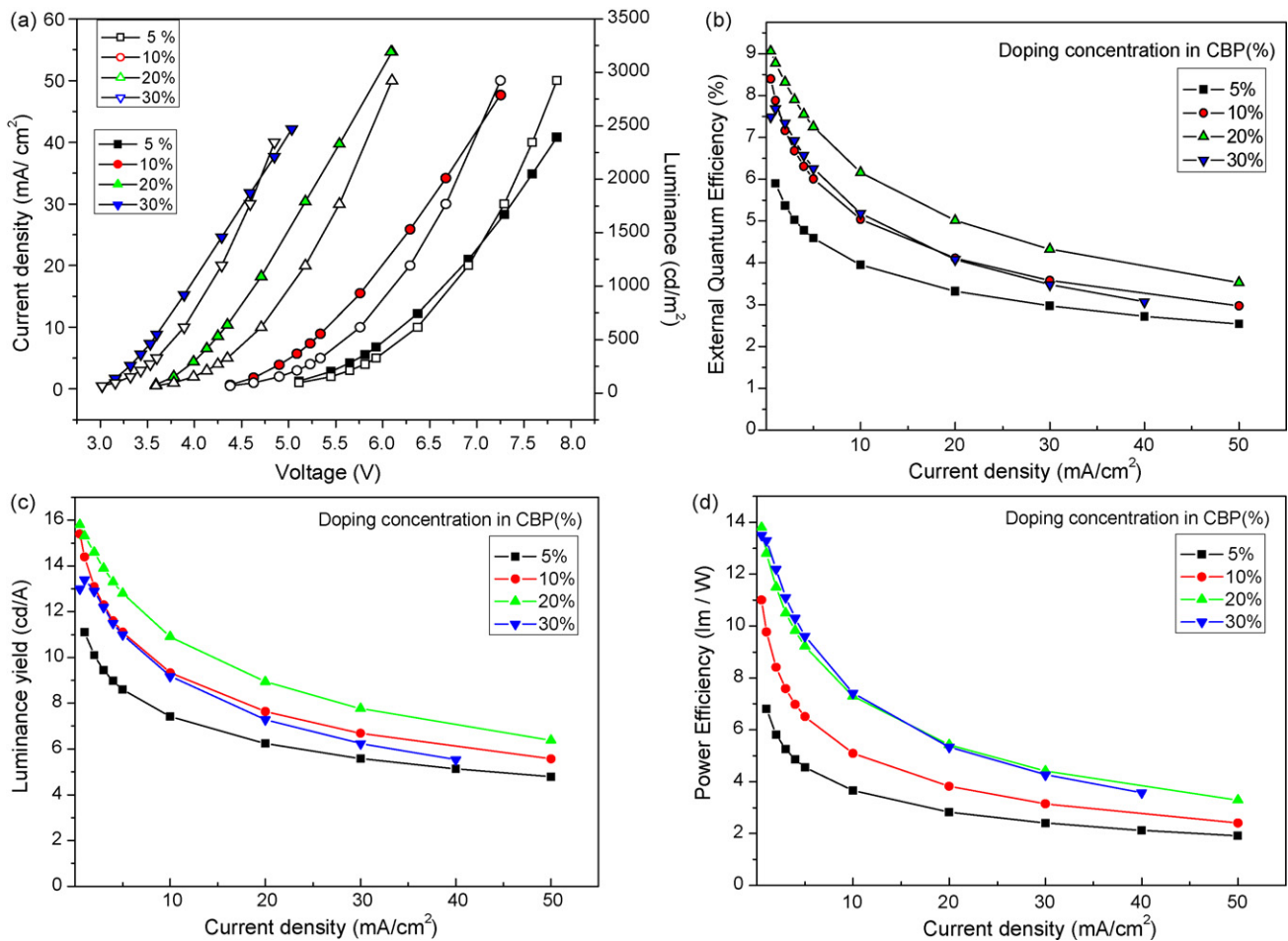
Fig. 3. (a) I–V–L curves for orange-red PHOLED devices (open symbols: current density; closed symbols: luminance); (b) external quantum efficiency; (c) luminance yield; (d) power efficiency versus current density curve with various doping concentrations of Ir(TBT)$_2$ (acac) in CBP.
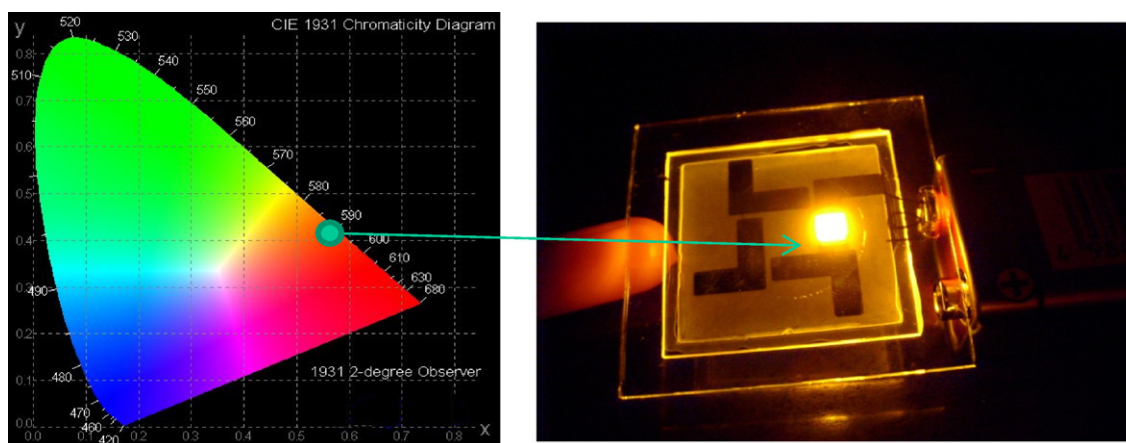
Fig. 4. The CIE coordinates of the orange-red PHOLED (20 wt.% dopant) with photograph of light emission.

of dopant results in ready capture of holes from NPB layer. As the concentration of $Ir(TBT)_2(acac)$ is increased, the efficiency of hole direct injection into dopant also enhances. The more balanced hole/electron recombination in emitter improves luminescent efficiency. Meanwhile, high doping level facilitates inter-dopant charge transfer with CBP acting as an inert host matrix, which offers an additional channel for charge transport and leads to the lower drive voltage [6,25,26].

The bulky triphenylamine group attached to benzotriazole effectively suppresses intermolecular interactions and alleviates self-quenching of the phosphorescence at high doping levels. For example, even when the dopant concentration arrived 30 wt.%, the luminance and power efficiencies are 13.39 cd/A and 13.32 lm/W with an external quantum efficiency of 7.69% at 1 mA/cm^2 (Fig. 3b, c and d). The low driving voltage and good efficiency of $Ir(TBT)_2(acac)$ make itself a strong candidate for efficient energy-saving white OELDs.

4. Conclusion

In summary, an amorphous iridium-benzotriazole phosphor $Ir(TBT)_2(acac)$ was studied as an orange-red PHOLED. It was found that low driving voltage and good efficiency orange-red PHOLED was realized with high doping concentration. Max luminance yield and EL efficiency of 20 wt.% doping concentration are about 15.81 cd/A and 9.06%, respectively, under which the operating voltage is 3.59 V (the CIE x, y coordinates $x = 0.58$, $y = 0.41$). The raise of doping concentration dramatically decreases driving voltage of CBP-based devices, which results in improved power efficiency. Our work is underway to use it as an orange-red phosphorescent dye in the fabrication of white OLEDs.

References

[1] B.W. D'Andrade, S.R. Forrest, Adv. Mater. 16 (2004) 1585.
[2] M.A. Baldo, M.E. Thompson, S.R. Forrest, Nature 403 (2000) 750.
[3] T. Nakayama, K. Hiyama, K. Furukawa, H. Ohtani, Society for Information Display (SID) International Symposium Digest, vol. 38, Long Beach, CA, 2007, p. 1018.
[4] W. Lu, B.X. Mi, M.C.W. Chan, Z. Hui, C.M. Che, N. Zhu, S.T. Lee, J. Am. Chem. Soc. 126 (2004) 4958.
[5] W.Y. Wong, Z. He, S.-K. So, K.L. Tong, Z. Lin, Organometallics 24 (2005) 4079.
[6] (a) Y.-L. Tung, L.-S. Chen, Y. Chi, P.-T. Chou, Y.-M. Cheng, E.Y. Li, G.-H. Lee, C.-F. Shu, F.-I. Wu, A.J. Carty, Adv. Funct. Mater. 16 (2006) 1615;
(b) Y.H. Niu, Y.L. Tung, Y. Chi, C.F. Shu, J.H. Kim, B. Chen, J. Luo, A.J. Carty, A.K.Y. Jen, Chem. Mater. 17 (2005) 3532.
[7] Y.L. Tung, S.W. Lee, Y. Chi, L.S. Chen, C.-F. Shu, F.-I. Wu, A.J. Carty, P.T. Chou, S.M. Peng, G.-H. Lee, Adv. Mater. 17 (2005) 1059.
[8] S.J. Yeh, M.F. Wu, C.T. Chen, Y.H. Song, Y. Chi, M.H. Ho, S.F. Hsu, C.H. Chen, Adv. Mater. 17 (2005) 285.
[9] D.K. Rayabarapu, B.M.J.S. Paulose, J.-P. Duan, C.-H. Cheng, Adv. Mater. 17 (2005) 349.
[10] Y.-H. Song, S.J. Yeh, C.T. Chen, Y. Chi, C.S. Liu, J.K. Yu, Y.-H. Hu, P.T. Chou, S.M. Peng, G.H. Lee, Adv. Funct. Mater. 14 (2004) 1221.
[11] H.Z. Xie, M.W. Liu, O.Y. Wang, X.H. Zhang, C.S. Lee, L.S. Hung, S.T. Lee, P.F. Teng, H.L. Kwong, H. Zheng, C.M. Che, Adv. Mater. 13 (2001) 1245.
[12] Y.G. Ma, H.Y. Zhang, J.C. Shen, Synth. Met. 94 (1998) 245.
[13] W.Y. Wong, C.-L. Ho, Z.-Q. Gao, B.-X. Mi, C.-H. Chen, K.W. Cheah, Z. Lin, Angew. Chem. Int. Ed. 45 (2006) 7800.
[14] J.J. Jiang, Y.H. Xu, W. Yang, R. Guan, Z.Q. Liu, H.Y. Zhen, Y. Cao, Adv. Funct. Mater. 17 (2007) 3580.
[15] (a) Z.W. Xu, Y. Li, X.M. Ma, X. Gao, H. Tian, Tetrahedron 64 (2008) 1860;
(b) Z.W. Xu, J. Tang, Q. Zhang, H. Tian, Chin. J. Lumin. 29 (2008) 578;
(c) E. Ishow, C. Bellaïche, L. Bouteiller, K. Nakatani, J.A. Delaire, J. Am. Chem. Soc. 125 (2003) 15744;
(d) J.F.K. Wilshire, Aust. J. Chem. 41 (1985) 1163;
(e) A. Recca, E. Libertini, P. Finocchiaro, H.S. Munro, D.T. Clark, Macromolecules 21 (1988) 2641;
(f) A.G. Koutsimpelis, Heterocycles 65 (2005) 1393;
(g) G.B. Liu, Adv. Synth. Catal. 349 (2007) 1637.
[16] (a) D. Tomkutė-Lukšienė, T. Malinauskas, A. StaniŠauskaitė, V. Getautis, K. Kazlauskas, P. Vitta, A. Žukauskas, S. Juršėnas, J. Photochem. Photobiol. A 198 (2008) 106;
(b) S. Thomas, US patent 20080015355 (2008).
[17] J.P. Duan, P.P. Sun, C.H. Cheng, Adv. Mater. 15 (2003) 224.
[18] X.M. Xu, H.S. Kwok, W.Y. Wong, G.J. Zhou, Chem. Mater. 18 (2006) 5097.
[19] Y.L. Tung, S.W. Lee, Y. Chi, Y.T. Tao, C.H. Chien, Y.M. Cheng, P.T. Chou, S.M. Peng, C.S. Liu, J. Mater. Chem. 15 (2005) 460.
[20] S.A. Van Slyke, C.H. Chen, C.W. Tang, Appl. Phys. Lett. 69 (1996) 2160.
[21] C. Reichardt, Solvents and Solvent Effects in Organic Chemistry, 2nd ed., VCH, Weinheim, 1990, pp. 339–387.
[22] Z.Q. Gao, M.M. Luo, X.H. Sun, H.L. Tam, M.S. Wong, B.X. Mi, P.F. Xia, K.W. Cheah, C.H. Chen, Adv. Mater. 21 (2008) 688.
[23] M.A. Baldo, C. Adachi, S.R. Forrest, Phys. Rev. B 62 (2000) 10967.
[24] J. Kalinowski, W. Stampor, J. Mezyk, M. Cocchi, D. Virgili, V. Fattori, P. Di Marco, Phys. Rev. B 66 (2002) 235321.
[25] C. Adachi, M.A. Baldo, M.E. Thompson, S.R. Forrest, J. Appl. Phys. 90 (2001) 5048.
[26] C.H. Wu, P.I. Shih, C.F. Shu, Y. Chi, Appl. Phys. Lett. 92 (2008) 233303.